RGNZ/MGPB

Geomechanical Response of Buner Marble, Pakistan, to Elevated Temperatures: Triaxial Strength Analysis through Single and Multistage Approaches

Rudarsko-geološko-naftni zbornik
(The Mining-Geology-Petroleum Engineering Bulletin)
UDC: 55: 552.1
DOI: 10.17794/rgn.2025.2.8

Original scientific paper

Asif Ali[1]; Waqas Ahmed[1]; Abdul Rahim Asif[1,2]*; Muhammad Yasir[1]; Ihtisham Islam[1,3]; Adnan Qadir[4]; Jehanzeb Khan[5]

[1]*National Centre of Excellence in Geology, University of Peshawar, Peshawar 25120, Pakistan.*
[2]*Department. of Geology, Fata University, FR Kohat, Pakistan.*
[3]*Department of Geology, Shaheed Benazir Bhutto University Sheringal, Dir Upper, 18030, Pakistan.*
[4]*Pakistan Museum of Natural History, Shakarparian National Park, Garden Ave, Islamabad, 44000, Pakistan.*
[5]*Department of Geology, University of Malakand, Chakdara, Dir (L) 18800, Pakistan.*

Abstract

This study investigates the effect of three-dimensional stress on the strength of marble from the Buner District, Khyber Pakhtunkhwa. It provides a comparative analysis of single and multi-stage triaxial tests to evaluate marble strength under ambient and elevated temperatures. Additionally, this study examines the physico-mechanical properties of the selected marble to enhance the understanding of its performance under varying conditions. A total of five bulk marble samples, (BM1 to BM5) were collected. From these samples, seventy (70) cores were extracted for the investigation of various physico-mechanical properties. Physical tests, including specific gravity, porosity, water absorption, and ultrasonic pulse velocity (UPV), as well as mechanical tests, such as unconfined compressive strength (UCS), unconfined tensile strength (UTS), point load test (PLT), and triaxial testing, were conducted. Physical properties were determined for five specimens (BM1 to BM5) selected from the bulk sample, while mechanical tests were carried out on the remaining 65 samples. Overall significant uniformity was observed in the values of all physico-mechanical properties except water absorption, which was found relatively higher in the case of BM3 and BM5 (0.093%) due to the increased amount of hydrophilic minerals in these samples. The remaining core specimens were treated at elevated temperatures (50°C, 75°C, 100°C, and 150°C). The mechanical properties including UCS, UTS, PLT, and triaxial tests were obtained on samples at ambient (25°C) and elevated temperatures. In the case of UCS and UTS, it was found that strength increases with an increasing temperature to a threshold temperature of 100°C, followed by a decrease at 150°C. Similarly, for the strength parameters (cohesion and friction angle) obtained during the triaxial tests, the threshold temperature was again found to be 100°C, thereafter strength degradation of the rocks occurred. The increase in strength is attributed to mineral thermal reactions causing the new bonding agents leading to the strengthening of rocks. Whereas, the decrease from 100°C to 150°C occurred due to the mineral thermal expansion resulting in thermal cracking and reduced strength. Based on the derived results, analysis, and their comparison with international standards, the studied rocks can be used for various underground construction purposes.

Keywords:
marbles; thermal treatment; physico-mechanical properties; single and multistage triaxial testing; thermal cracking

1. Introduction

Engineering design, construction, and related activities are significantly influenced by physical and mechanical properties. Due to their stability under a range of circumstances, including loads, moisture, and temperature exposures, different types of rock are used in engineering project (**Asif et al., 2022; Yasir et al., 2022; Ahmed et al., 2023; Nawaz et al., 2023; Bukhari et al., 2023; Shah et al., 2023; Asif et al., 2024**). Marbles are also utilized in a variety of global construction projects. The primary carbonate minerals that compose marble, a metamorphic rock, are calcite and/or dolomite. It is created when temperature and pressure are applied to dolomite or limestone. Calcium carbonate, which has several industrial applications, can be found in pure calcite marble. Calcite is the most prevalent and stable of the three polymorphs of calcium carbonate: aragonite (orthorhombic), vaterite (orthorhombic/hexagonal), and calcite (rhombohedral). Aragonite is rare and metastable, though it can change into calcite at temperatures between 300 and 400°C (**Plevová et al., 2010**). The use of natural stones like granite and marble in construction and decoration has led to a sharp rise in their extraction in recent years (**Silva et al., 2017; Kamran et al., 2022,**

* Corresponding author: Abdul Rahim Asif
e-mail address: abdulrahimasif@uop.edu.pk

Nawaz et al., 2023; Bukhari et al., 2023). Marble possesses unique engineering properties that impact its suitability as a construction material. Renowned for its durability, polished finish, wide array of attractive colors, and ease of processing, marble has been one of the most popular choices for construction and decorative stone since ancient times (**Raza et al., 2024**). Many researchers have determined the engineering properties of marbles (**Koroneos et al., 1980; Fahad et al., 2016; Peng et al., 2016; Rehman et al., 2022**).

Rock excavation in tunnel engineering has the potential to cause damage to a zone to varying degrees and upset the surrounding rock mass. Thus, when constructing tunnel support, understanding damage behaviour and deformation is crucial (**Yang et al., 2019; Khan et al., 2022, 2023**). In a deep tunnel excavation, lateral confinement unloading and vertical stress loading are applied to the surrounding rocks. These forces cause the surrounding rocks' mechanical qualities to deteriorate and sustain damage (**Zhang et al., 2021**). Triaxial rock tests have been carried out for many years in an effort to better understand how rocks behave under three-dimensional stress. According to **Hudson et al. (2014)**, the test aids in obtaining and validating mathematical expressions that are derived for the representation of rock behaviour in analytical and numerical models.

The triaxial test has recently gained popularity as a rock testing method in the field of rock mechanics. To better understand rock distortion, extensive experimental research has been done on a variety of rock types and loading scenarios. Triaxial compression tests were conducted by **Yang et al. (2008)** on marble fractures of various shapes. The findings demonstrated that the failure mechanisms and peak strengths rely on the fault geometry and confining pressure, and that the damaged and unbroken marbles exhibit distinct distortion features following peak stress**.** Granite samples taken from the Laizhou minefield in Shandong Province, China, were subjected to rock triaxial compression experiments by **Cai et al. (2015)**. The tests' objective was to use multistage triaxial tests to examine the mechanical reaction under various static stress circumstances. The findings demonstrated that while compressive strength increases as confining pressure rises, this rate falls as confining pressure rises. They also noted that failure is related to the stress rate in addition to the structure and material of the tested sample. At the same confining pressure, marble specimens' elastic, plastic, and strength behaviour were examined (**Yang et al., 2015**). The outcome demonstrated that marble's elastic modulus slowly declines with high axial stress but stays constant at lower axial deviatoric stress. On the other hand, as deviatoric stress increases, plastic modulus rapidly drops. Nevertheless, the tested marble's two moduli were independent of confining pressure. To examine stress-strain and acoustic properties, triaxial tests were conducted on marble at various confining pressures (**Cheng et al., 2021**). The findings demonstrated that while marble's elastic modulus and compressive strength increased and the specimen's failure mode shifted from splitting to shearing, the wave's amplitude and velocity reduced as confining pressure increased. **Yang et al. (2019)** examined mechanical behaviour with varying degrees of damage by conducting single and multi-stage triaxial tests on mudstone. The numerical results, both single and multistage, were in excellent agreement with the experimental findings.

Wang and Park (2002) used triaxial compression tests on sedimentary rocks to examine permeability for a full stress-strain process. The permeability of rocks varies as a result of deformation. Permeability was reduced at early loading and then increased as the specimen got closer to failure. When red sandstone was exposed to different temperatures, a series of triaxial compression tests revealed that the rock's strength rose between 20 and 200°C and fell between 200 and 600°C (**Yu et al., 2015**). In a similar manner, Tournemire shale's strength and deformation behaviour were examined at various temperature ranges, from 20 to 250°C, while maintaining confinement pressures between 0 and 20 MPa (**Masri et al., 2014**). As the temperature rose, the material's overall deformability increased, but Young's modulus and compression failure strength significantly decreased. Using triaxial compression tests following heat treatment from 200 to 600°C, **Zhu et al. (2021)** examined the deformation and strength properties of Nanan granite in Fujian Province, China. The findings indicated that at temperatures below 600°C, granite's volume rose by 4.11%, mass by 0.28%, and density by 4.21%. In contrast, from 500 to 600°C, strength decreased by 54.99%, elastic modulus by 39.8%, cohesiveness by 49.39%, and internal friction angle by 27.51%, respectively.

More than 3×10^9 tonnes of marble deposits can be found in Pakistan's northwest (**Shakirullah and Afridi, 2004; Fahad et al, 2016**). The first significant marble reserves in Pakistan were found by **Okrusch et al. (1976)** in the Mullagori and Swabi regions of Khyber Pakhtunkhwa (KP) Province. The main belts of marble occurrences found in KP are the southern district belt, the Mardan-Buner belt, the Swabi-Nowshera belt, and the Swat-Kohistan belt. Aside from these, the Reshun, Shoghore, Gahiret, and Shishi valleys of Chitral have been shown to contain enormous reserves (**Kazmi and Abbas, 2001; Bukhari et al., 2021). Fahad et al. (2016)** assessed the strength characteristics of marbles from Nowshera, Swabi, and Mardan, among other locations in Pakistan's Khyber Pakhtunkhwa. Characterizing the main forms of marble and comprehending how they behave when exposed to heat are urgently needed due to the deposits' varied geology and rising demand.

For the mining and construction sectors, it is crucial to use marble in a sustainable manner that is economically, ecologically, and socially viable. The demand for marble is primarily influenced by its lifespan (changes in

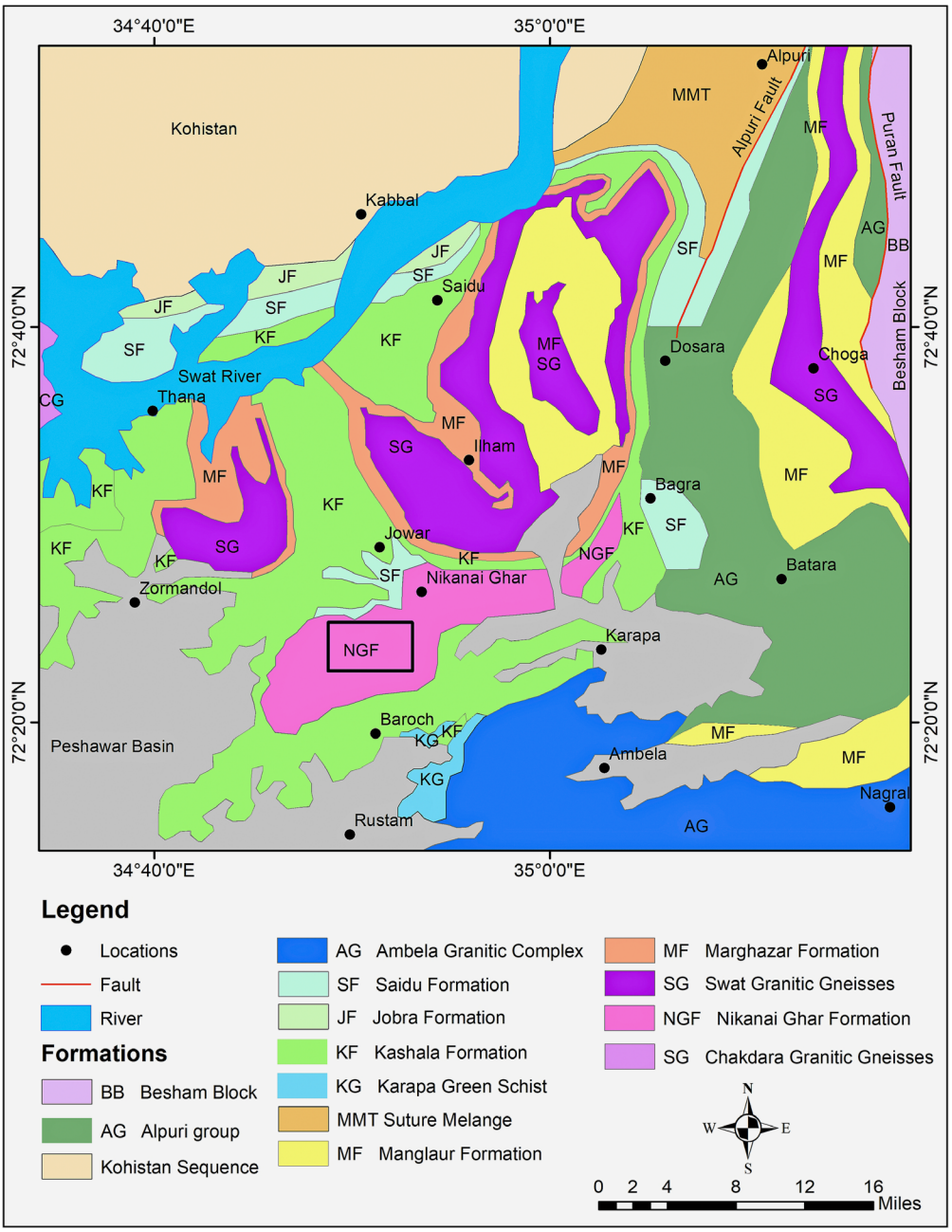

Figure 1: Regional geological map of the study area modified after **Hussain et al., 2004**

attributes due to heat exposure) and quality (physical and mechanical properties). This is particularly important for Pakistan's growing construction industry, supported by substantial untapped marble reserves. In the study area, significant infrastructure projects, such as a 1.45 km tunnel along the Buner motorway, are currently being planned. However, there has been limited research on the engineering characteristics of the rocks in this region. The study investigates the impact of heat on marble's peak compressive strength and overall mechanical properties. These findings hold academic significance and serve as a baseline for numerical analyses of tunnel excavation stability and other large-scale projects in the region.

2. Geological settings

The study area lies in the footwall of the Main Mantle Thrust (MMT) in the North-western Himalayas, which is a part of the active Himalayan foreland fold and thrust belt (see **Figure 1**). This Himalayan Mountain belt is formed due to the interaction of two continental Plates, India and Eurasia in the Ypresian period (**Calkins et al., 1975; Yeats and Hussain, 1987; Coward et al., 1988; Rowley, 1996; Shah et al., 2016).** This belt is characterized by intense folding, faulting, and thrusting of sedimentary, metamorphic, and igneous rocks, forming a series of linear mountain ranges and valleys. The belt is also known for its seismic activity, as the collision con-

tinues to drive crustal deformation and uplift in the Himalayas (**Ding et al., 2005**).

The Nikanai Ghar Formation, part of the Alpurai Group in Pakistan, consists primarily of medium- to high-grade metamorphic rocks such as schists, gneisses, and marbles. These rocks are thought to be of Proterozoic to Cambrian age and are characterized by extensive folding, faulting, and metamorphism due to tectonic activity associated with the Himalayan orogeny. The formation represents a sequence of sedimentary and volcanic precursors that underwent regional metamorphism.

The Nikanai Ghar Formation is named and described by **DiPietro, 1990**. The age of the Nikanai Ghar Formation is Triassic to the Jurassic (**DiPietro, 1990**). The contact between the Nikanai Ghar and Kashala formations is gradational and is placed above the last appearance of the micaceous rock in the Kashala Formation (see **Figure 1**). The contact with graphitic phyllites of the Saidu Formation is sharp. The proposed type locality is along stream valleys on the south side of Jafar Sar. Here, the Nikanai Ghar Formation consists of a thick-bedded sequence of dark grey to white marble and dolomitic marble with rare interlayers of graphitic phyllite and feldspathic quartzite. The marble is similar to that in the Kashala Formation, but coarsely crystalline varieties are more common. The major lithological difference between the two formations is the almost complete lack of micaceous rock in the Nikanai Ghar Formation. At its northeastern termination near Bagra, crystalline marble is interlayered with schistose marble and garnet-bearing calcareous schist. Beyond this point, the Nikanai Ghar Formation is not recognizable as a distinct lithological unit. In this area, it appears that the Nikanai Ghar Formation is interlayered with the Kashala Formation and underlies Saidu correlatives at Bagra (**DiPietro et al., 1993**).

3. Material and methods

The focus of the research is to provide a detail of methods adopted to obtain the physical and mechanical properties of Buner marbles and to establish a possible relationship between these properties at ambient and elevated temperatures of 50°C, 75°C, 100°C, and 150°C. Further, the conventional single and multistage triaxial compression tests are performed at ambient conditions (25°C) and after heat treatment (50°C, 75°C, 100°C, and 150°C) at a heating rate of 5°C/ minute. The chosen temperatures (25°C, 50°C, 75°C, 100°C, and 150°C) were selected to represent a range that could effectively capture the thermal behavior and strength response of the marble samples. The baseline temperature of 25°C was used to represent the ambient condition, while the incrementally higher temperatures allowed for the observation of changes in mechanical properties up to the threshold where significant strength degradation was noted. The upper limit of 150°C was chosen based on typical temperature ranges encountered in natural and engineering settings, providing insight into the marble's performance under elevated conditions relevant to construction and geological processes.

Detailed fieldwork was arranged in the Buner area. An accessible body of marble deposits occurs in the study area. These marble deposits display a variety of colors from white to grey to white with dark bends. The collected samples' location lies at latitude 34°28'52.08" N and longitude 72°16'2.05" E in Buner District, Malakand Division of Khyber Pakhtunkhwa, Pakistan (see **Figure 1**). A minimum of one cubic foot ($1ft^3$) of five Bulk rock samples (BM1, BM2, BM3, BM4, and BM5) were collected from the Nikani Ghar Formation, Buner area. The samples were selected based on textural and lithological similarities for Physico-mechanical evaluations. During the collection of bulk samples, it was confirmed that the samples were free from cracks and other discontinuities. Calcite precipitation was found very common in the cracks within the Marble deposits. Scaled photographs were taken in the field. Samples were extracted from the outcrops systematically and brought to the National Centre of Excellence in Geology, the University of Peshawar for a detailed geotechnical investigation.

For the determination of physico-mechanical properties, a total of five (5) cylindrical core specimens (108 mm in length and 54 mm in diameter) were obtained from each bulk sample (see **Figure 2**), adhering to a length-to-diameter ratio of 2:1. These dimensions were selected in accordance with ASTM D4543 standards to ensure consistency and reliability in the testing of physico-mechanical properties. This amounted to a total of 60 core specimens. Cores were extracted using a core drilling machine in the thin section preparation laboratory of the National Centre of Excellence in Geology, University of Peshawar. The extracted cores were large from the required sizes and the sides were cut later to obtain the required length using a rock-cutting machine and smoothed with a small-scale grinder as given by the ASTM C170/C170M-16. The samples were tested in a dry state. Before testing, they were oven-dried at 105°C for 24 hours to remove any moisture content, ensuring uniform initial conditions and consistency across all tests.

The physical tests such as specific gravity, water absorption, and porosity were performed on the rock cores following the ASTM C170/C170M-16. P wave velocity (UPV) was measured using ultra-sonic pulse velocity equipment (UPV) before and after the heat treatment. After the completion of physical tests, mechanical tests such as unconfined compressive strength (ASTM C170/C170M-17) and unconfined tensile strength (ASTM D 3967-16), point load strength index (ASTM D 5731). The Schmidt Hammer Test (SHT) test was conducted to calculate the R-values, which were used to assess the strength of a rock sample (ASTM, D5873-14). For SHT,

Figure 2: Cylindrical core samples of Buner Marbles, Pakistan

L-type Schmidt hammer was employed in this research. The L-type hammer is designed specifically for testing low-strength rocks and has an impact energy of 0.735 Nm, lower than that of the N-type hammer, making it suitable for the studied limestones.

Triaxial tests offer significant advantages for understanding the behavior of rocks under stress by closely simulating real-world conditions. These tests replicate in-situ stress environments by applying controlled confining pressure, which allows researchers to study how rocks respond to the stresses they would naturally experience in subsurface settings. This is particularly useful for evaluating rock stability in various engineering and construction scenarios.

One of the key benefits of triaxial tests is their ability to determine critical strength parameters such as cohesion and the angle of internal friction. These parameters are essential for assessing rock stability and designing structures like foundations, tunnels, and slopes. Additionally, triaxial tests provide a detailed stress-strain response, capturing the behavior of rocks during elastic deformation, plastic deformation, and eventual failure. This helps engineers and geologists understand the complete mechanical behavior of the material under varying pressure conditions.

Moreover, triaxial tests are valuable for studying the anisotropy and heterogeneity of rocks. By testing samples in different orientations, researchers can evaluate the impact of mineral alignment or fabric on rock strength and deformation. These tests also help predict failure mechanisms, such as shear or tensile failure, and provide insight into fracture patterns, which are critical for ensuring safety and stability in geotechnical projects. Triaxial tests were performed on core samples having NX size (54 mm) and were extracted from the bulk samples from (BM1 to BM5) following the suggested method of the International Society for Rock Mechanics (ISRM). Core samples were heated in the oven at a temperature of 50°C, 75°C, 100°C, and 150°C for 24 hours and then cooled down in the oven to avoid sudden thermal shocks. These heat-treated samples were given specific heat levels: Level 1 (25°C-Ambient), Level 2 (50°C), Level 3 (75°C), Level 4 (75°C) and Level 5 (150°C). Four specimens were tested for each level of temperature during triaxial testing; three for the single stage and one for the multi-stage triaxial test (see **Table 1**).

The ISRM has suggested three test types for the determination of rock failure envelope such as single-stage triaxial test (SST), multi-stage triaxial test (MST), and continuous failure state (MFS) (**Csuhanics and Debreczeni, 2013**). In this study, all the tests were performed using the procedures of the first two types (i.e. SST and MST). For each test, the core specimen was initially injected into the Hoek triaxial cell and lateral stress was applied at a rate of 0.20 MPa. The specimen was adjusted in the cell and placed in a compression machine (having a capacity of 3000 kN) and the axial load was applied at a rate of 0.5 MPa/second (see **Figure 3**). When the sample started taking the axial load, the target confining stress was applied (2, 4, and 6 MPa). In the case of the single-stage triaxial test, three separate specimens were used for each confining stress, whereas, in the case of the multi-stage triaxial test a single specimen was used and the target confining stresses were applied. The confining stress was applied with the help of a hydraulic pump having mineral oil inside. While performing both single and multistage triaxial tests, continuous measurements of axial loads, confining pressure, and displacement linear variable differential transducers (LVDT) were taken. The target confining pressures were achieved by simultaneously increasing lateral stress and axial stress. This followed by progressively increasing the axial stress till the sample was failed. For multistage triaxial tests, a single specimen was tested with 3 stages of increasing confining pressures i.e. 2, 4, 6 MPa. The

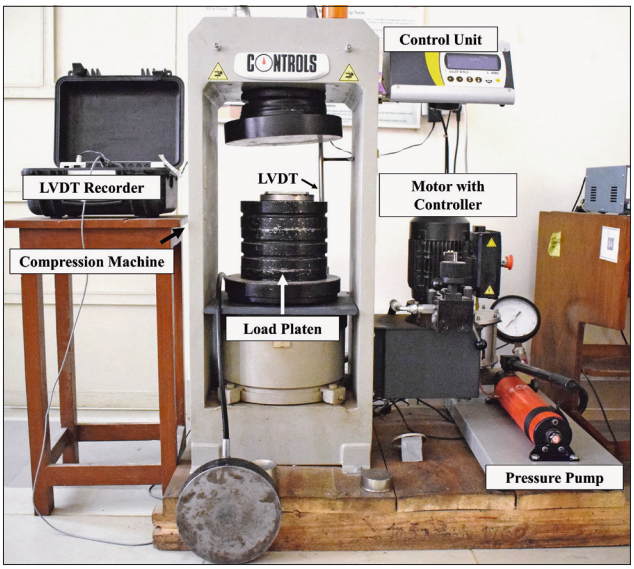

Figure 3: Compression machine along with LVDT, and pressure pump used in triaxial testing

Table 1: Testing plan followed during the research work

Temperature (C°)	Sample	Specimen designation	Confining pressure (MPa)	Test type
25 (ambient)	BM1	BM1a	2, 4, 6	MST
		BM1b	2	SST
		BM1c	4	
		BM1d	6	
		BM1e	--	UCS
		BM1f	--	UTS
		BM1g	--	PL
50	BM2	BM2a	2, 4, 6	MST
		BM2b	2	SST
		BM2c	4	
		BM2d	6	
		BM2e	--	UCS
		BM2f	--	UTS
		BM2g	--	PL
75	BM3	BM3a	2, 4, 6	MST
		BM3b	2	SST
		BM3c	4	
		BM3d	6	
		BM3e	--	UCS
		BM3f	--	UTS
		BM3g	--	PL
100	BM4	BM4a	2, 4, 6	MST
		BM4b	2	SST
		BM4c	4	
		BM4d	6	
		BM4e	--	UCS
		BM4f	--	UTS
		BM4g	--	PL
150	BM5	BM5a	2, 4, 6	MST
		BM5b	2	SST
		BM5c	4	
		BM5d	6	
		BM5e	--	UCS
		BM5f	--	UTS
		BM5g	--	PL

first loading stage was the same as for single-stage triaxial loading. After achieving the confining pressure, the axial load was increased until rock failure occurred, and the axial load was stopped. The confining pressure was then increased up to the next level and the same procedure was repeated till the failure of the rock occurred.

4. Results and discussion

The physico-mechanical characteristics of intact rocks are thought to be the most crucial factors for the design and construction of engineering projects including tunnels, underground structures, dams, rock slopes, foundations on rock, and dams (**Yaşar and Erdoğan, 2004**). The American Society for Testing and Materials (ASTM) and the International Society for Rock Mechanics (ISRM) have standardised the measurement of rock strength. It is very important to explain how heat affects natural building materials in addition to their physico-mechanical characteristics. The strength characteristics and deformation characteristics of rock at high temperatures are relevant to civil engineering, geology, energy, safe coal seam drainage, mining and underground storage of natural gas and petroleum, efficient use of geothermal resources, and comprehensive utilization (**Ali et al., 2023; Janjuhah et al., 2021a**). According to **Yavuz et al. (2010)**, the fundamental determinants of the physical characteristics of rocks are geometry and crack density. According to **Tian et al. (2017)**, granite's UCS reduces significantly after 400°C, yet it only marginally changes from room temperature to that point (**Liu and Xu, 2015**). After a particular temperature threshold, many researchers discovered that rocks exposed to high temperatures exhibited a decline in their strength and deformation characteristics (**Chen et al., 2012; Ding et al., 2016; Peng et al., 2016**). Marble, siltstone, coal, and limestone all underwent mechanical testing such as uniaxial and triaxial tests, which showed that they absorbed energy under loading conditions before releasing it after reaching their maximum strength (**He et al., 2010**). For operations like the disposal of deep geological nuclear waste, an understanding of the mechanical behaviour of rocks at ambient and high temperatures is crucial. Thus, the physicomechanical characteristics of the core samples taken from the study area were assessed both before and after heat treatment in the current investigation. This section discusses the measured physico-mechanical results, which are provided in the corresponding tables.

4.1. Physical properties

4.1.1. Specific gravity

The strength of rocks is significantly influenced by their physical properties, which is crucial for various construction applications. A decrease in rock strength can adversely affect the engineering characteristics of any project. In this study, specific gravity was measured for five specimens, labeled BM1 to BM5, with the results presented in **Table 2**. The specific gravity for all specimens was consistently around 2.71, except for BM3, which measured 2.72. According to **Blyth and De Freitas (1974)**, a specific gravity greater than 2.55 indicates that the rock is suitable for heavy construction.

Table 2: Results of physical properties of the studied rock samples

Sample No.	Weight in air (g)	Weight in water (g)	SSD weight (g)	Dry weight (g)	Specific gravity	Porosity (%)	Water absorption (%)
BM-1	687.69	434.04	687.78	687.20	2.71	0.19	0.084
BM-2	690.57	435.86	690.88	690.27	2.71	0.12	0.088
BM-3	685.75	432.87	685.91	685.27	2.72	0.19	0.093
BM-4	688.43	434.50	688.52	688.10	2.71	0.13	0.060
BM-5	686.89	433.59	687.07	686.43	2.71	0.18	0.093

Table 3: Ultrasonic pulse velocity of studied samples at various degrees of temperature

Temperature °C	Sample No.	Specimen No.	Length (m)	Time (µs)	UPV (m/s)	UPV (m/s) average
Ambient	BM1e	BM1e-1	0.108	33.12	3260.87	3253.34
		BM1e-2	0.108	33.26	3247.14	
		BM1e-3	0.108	33.21	3252.03	
50	BM2e	BM2e-1	0.112	39.85	2810.54	2791.1
		BM2e-2	0.113	39.97	2827.12	
		BM2e-3	0.110	40.21	2735.64	
75	BM3e	BM3e-1	0.115	44.93	2559.54	2532.82
		BM3e-2	0.112	45.10	2483.37	
		BM3e-3	0.115	45.00	2555.56	
100	BM4e	BM4e-1	0.111	48.95	2267.62	2271.77
		BM4e-2	0.109	48.77	2234.98	
		BM4e-3	0.113	48.86	2312.73	
150	BM5e	BM5e-1	0.116	45.89	2527.78	2540.06
		BM5e-2	0.118	45.72	2580.93	
		BM5e-3	0.115	45.79	2511.47	

Therefore, based on the specific gravity results of the studied samples, these rocks are deemed appropriate for heavy construction applications, including tunnels and underground storage reservoirs.

4.1.2. Water absorption

Water absorption refers to the amount of water contained within a rock. Key factors influencing a rock's physical properties include pore structure, crack geometry, and crack density. A high-water absorption value typically correlates with lower rock strength, and even a slight increase in water content can lead to a significant reduction in strength (**Erguler and Ulusay, 2009**). **Table 2** presents the water absorption values for the studied Buner marble specimens (BM1 to BM5), which ranged from 0.060% to 0.093%. The relatively higher water absorption in BM2 and BM4 suggests an increased presence of hydrophilic minerals compared to the other samples. These findings align with the research by **Fahad et al. (2016)**, which indicated that the marbles from the Nikani Ghar Formation (Buner marble) exhibited lower water absorption values than those specified by internationally accepted ASTM standards.

Higher water absorption rates in marble samples can significantly impact their durability and weathering resistance when used in outdoor structures. Increased water absorption can lead to greater susceptibility to weathering processes, such as freeze-thaw cycles, where water within the pores expands and contracts as temperatures fluctuate. This expansion can cause cracking and structural degradation over time. Additionally, higher water absorption may enhance the dissolution of minerals, leading to surface erosion and a reduction in the overall mechanical integrity of the rock. Therefore, samples with higher water absorption rates are more likely to experience accelerated weathering and reduced lifespan when exposed to outdoor environmental conditions.

4.1.3. Porosity

Porosity is one of the most important parameters that influence weathering and therefore the durability of construction material (**Barone et al., 2015**). The factors that control porosity are grain size, shape, and mineralogical composition (**Sajid et al., 2016; Janjuhah et al., 2021b**). Rock strength is inversely proportional to porosity and related to the shape and size of pores. The results of the porosity of study samples coincide with the values of water absorption as shown in **Table 2**. The porosity of five specimens was measured which ranged from 0.12 % to 0.19% from BM2 to BM1.

Table 4: Unconfined compressive strength result of studied samples at various degrees of temperature

Temperature °C	Sample No.	Specimen No.	Dia. (m)	Length (m)	Area (m^2)	Load (kN)	UCS (MPa)	Average UCS (MPa)
Ambient	BM1e	BM1e-1	0.054	0.108	0.0023	90.0	39.00	36.89
		BM1e-2	0.054	0.108	0.0023	86.0	37.16	
		BM1e-3	0.054	0.108	0.0023	79.0	34.51	
50	BM2e	BM2e-1	0.056	0.112	0.0024	113.1	46.61	43.52
		BM2e-2	0.055	0.113	0.0024	109.0	46.19	
		BM2e-3	0.055	0.110	0.0024	90.7	37.78	
75	BM3e	BM3e-1	0.056	0.115	0.0024	116.3	47.92	47.11
		BM3e-2	0.055	0.112	0.0024	117.1	48.78	
		BM3e-3	0.056	0.115	0.0024	108.0	44.50	
100	BM4e	BM4e-1	0.056	0.111	0.0024	130.8	53.84	51.94
		BM4e-2	0.056	0.109	0.0024	120.7	49.92	
		BM4e-3	0.056	0.113	0.0025	128	52.07	
150	BM5e	BM5e-1	0.056	0.116	0.0024	116.2	47.49	47.71
		BM5e-2	0.056	0.118	0.0025	114	46.09	
		BM5e-3	0.055	0.115	0.0024	119	49.57	

4.1.4. Ultra-Sonic pulse velocity

In this study, the ultrasonic pulse velocity for the studied samples at various heating temperatures (25, 50, 75, 100, and 150ºC) and for a duration of 24 hours were examined. In the laboratory, P wave velocity was used to characterize and determine the effects of time and temperature treatments. From **Table 3**, it can be observed that the heat treatment has a significant impact on ultrasonic pulse velocity. UPV values continuously decrease when the temperature increases from ambient to 100ºC because more dissociation occurs in the rock samples. However, then for 150ºC, the UPV values increased slightly which showed that the sensitivity of UPV to discontinuities caused a change in rock samples.

4.2. Strength properties

4.2.1. Unconfined compressive strength

The UCS is a crucial parameter that reflects the fundamental mechanical properties of rocks, playing a vital role in rock mass classification and the development of failure criteria for rocks and rock masses (**Jaeger et al., 2007; Asif et al., 2021; Yasir et al., 2022; Ahmed et al., 2023; Asif et al., 2024**). In this study, UCS values were measured on a total of fifteen core specimens across various temperatures, with three specimens tested for each temperature increment from ambient conditions up to 150ºC. The results are summarized in **Table 4**.

The average strength showed a gradual increase from ambient temperature to 100°C, rising from 36.89 MPa to 51.94 MPa for samples BM1e to BM4e. However, at 150°C, the strength of sample BM5e decreased compared to the other samples measured from ambient to 100°C. This reduction in strength is attributed to the increase in grain size and the development of fractures caused by heat treatment. Consequently, based on the UCS results of the studied samples, these rocks are deemed suitable for heavy construction applications, such as tunnels and underground storage reservoirs.

4.2.2. Unconfined tensile strength

High temperatures within rocks lead to thermal expansion and reactions, resulting in significant alterations to microstructures, such as micro-cracks and mineral bond changes. The heating and cooling processes during thermal treatment can inflict considerable thermal damage on rock samples. In this study, the average UCS and UTS values of the marble samples soaked in water were found to be lower than those of the rock core samples that were cooled in the oven. To mitigate additional thermal shock, we opted to cool the marble samples in the oven. Tensile strength values were measured continuously from the natural state up to 150°C, and the results are presented in **Table 5**. The average tensile strength values increased from 6.01 MPa at ambient temperature to 7.17 MPa at 100°C, attributed to the reduction of continuous fractures and the closure of grain boundaries resulting from the thermal expansion of calcite minerals. However, at 150°C, there was a slight decrease in tensile strength due to the increased dissolution of cavities and the opening of cracks. Among the samples tested, the BM4f sample demonstrated greater stability compared to the other marble specimens.

4.2.3. Point load

In this study, the point load tests were performed on specimens from (BM1g to BM5g) from ambient tem-

Table 5: Unconfined tensile strength result of studied samples at various degrees of temperature

Temperature	Sample No.	Specimen	Dia (mm)	R=D/2	Thickness (mm)	Area=(πRT)	UTS (MPa)	Average (MPa)
Ambient	BM1f	BM1f-1	54.4	27.2	25.2	2152.28	6.20	6.01
		BM1f -2	54.2	27.1	25.1	2135.86	6.12	
		BM1f -3	54	27	25.3	2144.93	5.72	
50°C	BM2f	BM2f -1	54.3	27.15	25.2	2148.33	6.39	6.33
		BM2f -2	54.4	27.2	25.4	2169.36	6.32	
		BM2f -3	54	27	25.2	2136.46	6.28	
75°C	BM3f	BM3f -1	54.4	27.2	25.3	2160.82	6.79	6.90
		BM3f -2	54.2	27.1	25.1	2135.86	7.02	
		BM3f -3	54.2	27.1	25.3	2152.88	6.91	
100°C	BM4f	BM4f -1	54.4	27.2	25.2	2152.28	7.32	7.17
		BM4f -2	54.2	27.1	25.2	2144.37	6.76	
		BM4f -3	54	27	25.4	2153.41	7.43	
150°C	BM5f	BM5f -1	54	27	25.2	2136.46	6.81	6.78
		BM5f -2	54.4	27.2	25.1	2143.74	6.52	
		BM5f -3	54.2	27.1	25.3	2152.88	7.01	

Table 6: Results of point load test of studied rocks at various degrees of temperature

Temperature	Sample No.	Specimen	D	L	D2	P(kN)	IS	F	Is50	Average
Ambient	BM1	BM1g-1	54	27.3	2916	7.15	2.45	1.04	2.54	2.49
		BM1g-2	54	27.4	2916	6.81	2.34	1.04	2.42	
		BM1g-3	54	27.1	2916	7.09	2.43	1.04	2.52	
50°C	BM2	BM2g-1	54	27.7	2916	3.87	1.33	1.04	1.37	1.97
		BM2g-2	54	27.6	2916	6.16	2.11	1.04	2.19	
		BM2g-3	54	27.4	2916	6.66	2.28	1.04	2.36	
75°C	BM3	BM3g-1	54	27.2	2916	6.08	2.09	1.04	2.16	1.93
		BM3g-2	54	27.5	2916	4.28	1.47	1.04	1.52	
		BM3g-3	54	27.8	2916	6.00	2.06	1.04	2.13	
100°C	BM4	BM4g-1	54	27.6	2916	5.95	2.04	1.04	2.11	2.05
		BM4g-2	54	27.7	2916	5.80	1.99	1.04	2.06	
		BM4g-3	54	27.1	2916	5.64	1.93	1.04	2.00	
150°C	BM5	BM5g-1	54	27.4	2916	5.60	1.92	1.04	1.99	1.92
		BM5g-2	54	27.5	2916	5.27	1.81	1.04	1.87	
		BM5g-3	54	27.2	2916	5.38	1.84	1.04	1.91	

peratures up to 150°C. The results are given in **Table 6**, which shows a continuous decrease in point load strength from ambient to 150ºC. The highest average strength value was measured for BM1g at ambient temperature and the lowest strength value was for BM5g at 150°C. Similar studies were reported by **Labeeb et al. (2021)** on intact rocks such as granite, sandstone, marble, and limestone at a temperature ranging from 25ºC to 1100°C, the results showed that as with temperature, the point load index of rocks decreased.

4.2.4. Schmidt hammer

Table 7 shows the average reading (R) of each sample's ten impacts at different locations (R1 to R10). The rebound R-value ranged from 39.3 for BM2 to 40.5 for BM3.

4.2.5. Triaxial testing

In this study, five temperature levels were monitored, ranging from ambient conditions (Level 1) to 150°C (Level 5). For each temperature level, four tests were conducted: one multistage test and three single-stage tests. These triaxial experiments were performed under confining pressures of 2, 4, and 6 MPa. In the single-stage triaxial tests, three specimens were evaluated at each confining pressure, while a single specimen was used for the multistage test at the same pressures. The maximum axial stress (in MPa) was recorded for both the

Table 7: Results of Schmidt hammer of bulk samples

Sample No.	R1	R2	R3	R4	R5	R6	R7	R8	R9	R10	R (Average)
BM1	40	38	42	36	39	37	43	36	43	40	39.4
BM2	37	39	41	40	43	38	36	37	40	42	39.3
BM3	43	39	44	42	38	37	36	41	42	43	40.5
BM4	42	40	41	38	41	39	39	37	40	40	39.7
BM5	41	39	42	38	43	37	35	39	38	43	39.5

Table 8: showing the results of MT tests performed on BM

Sample designation: BM1a (Level-1-25°C)					
Dimensions		Stages			
Día (mm)	55.83		1	2	3
Length (mm)	114.5	Confining pressure (MPa)	2	4	6
Area (mm^2)	2446.8	Axial stress (MPa)	53.08	70.74	81.73
		Angle of internal friction	48.12°		
		Cohesion	0.83 MPa		
Sample designation: BM2a (Level-2-50°C)					
Dimensions		Stages			
Día (mm)	55.6		1	2	3
Length (mm)	111	Confining pressure (MPa)	2	4	6
Area (mm^2)	2426.71	Axial stress (MPa)	45.74	53.98	70.62
		Angle of internal friction	39.35°		
		Cohesion	0.82 MPa		
Sample designation: BM3a (Level-3-75°C)					
Dimensions		Stages			
Día (mm)	56.3		1	2	3
Length (mm)	109	Confining pressure (MPa)	2	4	6
Area (mm^2)	2488.2	Axial Stress (MPa)	52	69.84	82.9
		Angle of internal friction	46.97°		
		Cohesion	0.81 MPa		
Sample designation: BM4a (Level-4-100°C)					
Dimensions		Stages			
Día (mm)	55.93		1	2	3
Length (mm)	111.2	Confining pressure (MPa)	2	4	6
Area (mm^2)	2455.6	Axial stress (MPa)	68.29	83.35	95
		Angle of internal friction	43.98°		
		Cohesion	0.83 MPa		
Sample designation: BM5a (Level-5-150°C)					
Dimensions		Stages			
Día (mm)	55.3		1	2	3
Length (mm)	111	Confining pressure (MPa)	2	4	6
Area (mm^2)	2400.6	Axial stress (MPa)	43.65	49.77	58.32
		Angle of internal friction	38°		
		Cohesion	0.66 MPa		

Table 9: showing the results of ST tests performed on BM

Sample designation: BM1b, BM1c, BM1d (Level-1-25°C)							
Dimensions	Specimen				Stages		
	1	2	3		1	2	3
Día (mm)	55.86	56.36	55.96	Confining pressure (MPa)	2	4	6
Length (mm)	115.5	113.5	115.5	Axial stress (MPa)	55.14	57.12	81.96
Area (mm^2)	2449.46	2493.51	2458.24	Angle of internal friction (deg)	44°		
				Cohesion (MPa)	0.76		
Sample designation: BM2b, BM2c, BM2d (Level-2-50°C)							
Dimensions	Specimen				Stages		
	1	2	3		1	2	3
Día (mm)	55.83	56	57	Confining pressure (MPa)	2	4	6
Length (mm)	115.3	113	114.2	Axial stress (MPa)	56.34	54.53	76.05
Area (mm^2)	2446.26	2461.76	2550.46	Angle of internal friction (deg)	43.92°		
				Cohesion (MPa)	0.76		
Sample designation: BM3b, BM3c, BM3d (Level-3-75°C)							
Dimensions	Specimen				Stages		
	1	2	3		1	2	3
Día (mm)	56	55.9	55.8	Confining pressure (MPa)	2	4	6
Length (mm)	111.3	114.2	111.3	Axial stress (MPa)	69.92	81.07	92.78
Area (mm^2)	2461.76	2452.97	2444.2	Angle of internal friction (deg)	43.02°		
				Cohesion (MPa)	0.75		
Sample designation: BM4b, BM4c, BM4d (Level-4-100°C)							
Dimensions	Specimen				Stages		
	1	2	3		1	2	3
Día (mm)	56	56.13	56.2	Confining pressure (MPa)	2	4	6
Length (mm)	113.6	114.6	113.5	Axial stress (MPa)	46.43	72.03	74.86
Area (mm^2)	2461.76	2473.2	2461.76	Angle of internal friction (deg)	51.3°		
				Cohesion (MPa)	0.89		
Sample designation: BM5b, BM5c, BM5d (Level-5-150°C)							
Dimensions	Specimen				Stages		
	1	2	3		1	2	3
Día (mm)	55.93	55.93	56	Confining pressure (MPa)	2	4	6
Length (mm)	112	114	111	Axial stress (MPa)	33..51	45.47	55.61
Area (mm^2)	2455.6	2455.6	2461.76	Angle of internal friction (deg)	41.45°		
				Cohesion (MPa)	0.72		

multistage and single-stage tests under the selected confining pressures. Additionally, the angle of internal friction (in degrees) and cohesion (in MPa) were measured.

During the triaxial tests, two types of cracks developed in the rock core specimens: wing cracks, which occur along the shear plane or the direction of maximum principal stress, and secondary cracks, which form above or below the shear plane or along its boundaries (**Yang et al., 2008**). As confining pressure increases, the brittleness of the rock sample decreases, causing a transition in

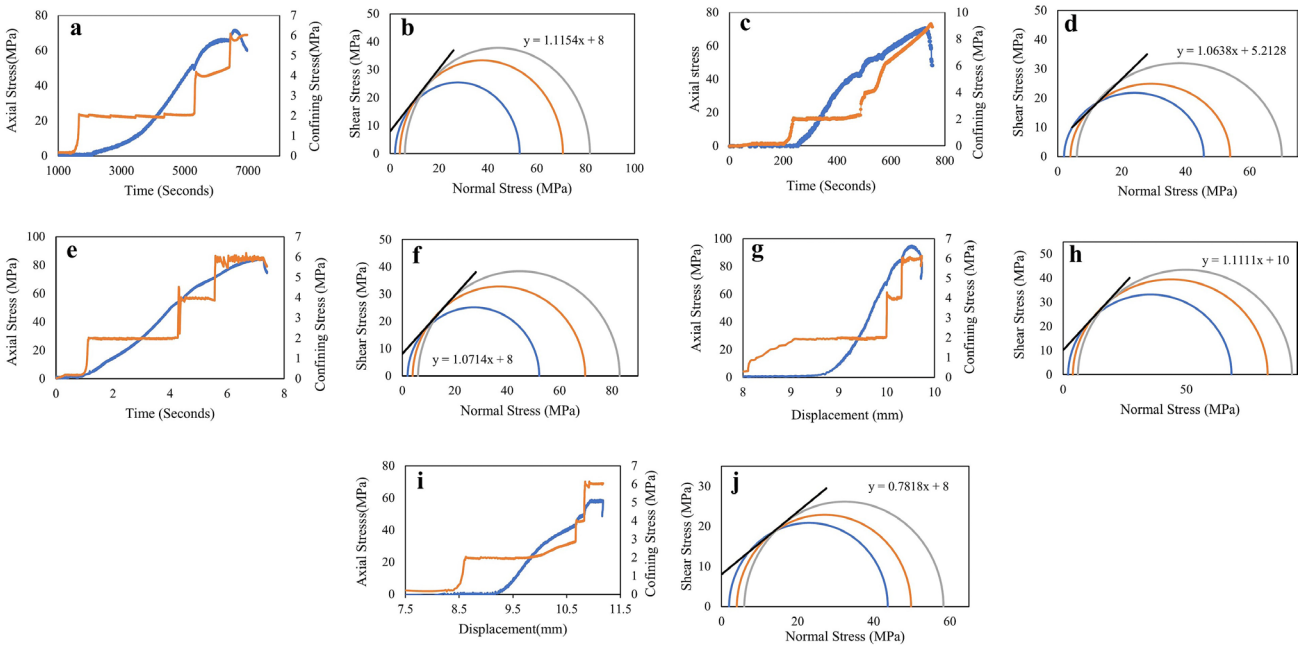

Figure 4 (a-j): shows the Stress paths of multi-stage triaxial (MST) testing and Mohr's circle diagram at various temperatures. **a** and **b** show the Stress paths of MST and Mohr's circle diagram at 25°C; **c** and **d** show the Stress paths of MST and Mohr's circle diagram at 50°C; **e** and **f** show the Stress paths of MST and Mohr's circle diagram at 75°C; **g** and **h** show the Stress paths of MST and Mohr's circle diagram at 100°C; **i** and **j** show the Stress paths of MST and Mohr's circle diagram at 150°C. The blue line depicts axial stress, and the orange line shows confining stress.

failure modes from tension-splitting to mixed tension-shear failure and ultimately to shear failure (**Zhang et al., 2021**). The maximum axial stress observed during testing reflects the triaxial compressive strength corresponding to the specific confining pressure applied. The ability of the rock to withstand shear stress is indicated by the angle of internal friction (φ). It was noted that as the angle of internal friction increases, the cohesion of the rock decreases, resulting in a change in the rock's behavior from brittle to ductile.

Overall, the results indicate that thermal effects reduce the brittleness of the rock specimens while enhancing ductility. Furthermore, the findings demonstrate that high confining pressure diminishes the impact of thermal effects on the mechanical properties of the studied rock, while elevated temperatures enhance the influence of confining pressure. Similar conclusions were drawn by **Meng et al. (2017)** in a study examining the effects of temperature on the mechanical properties of slates under triaxial compression tests at confining pressures of 5, 10, 15, 20, and 25 MPa, with temperatures of 20, 40, 80, and 120°C. All the triaxial tested samples according to their level of temperature are discussed in the following section.

Level 1 (25°C)

At ambient temperature, four triaxial tests were conducted. In the multistage triaxial test with a confining pressure of 2 MPa, the maximum axial stress recorded was 53.08 MPa (see **Table 8; Figures 4a and 4b**). When the confining pressure was increased to 4 MPa, the peak axial stress rose to 70.74 MPa. Finally, at a confining pressure of 6 MPa, the peak axial stress reached 81.73 MPa (see **Table 8; Figures 4a and 4b**). In the single-stage triaxial tests for confining pressures of 2, 4, and 6 MPa, the axial stresses measured were 55.14, 57.12, and 81.96 MPa, respectively (see **Table 9; Figures 5 a-d**).

Notably, the axial stress for the 4 MPa confining pressure was lower than that of the other samples (as discussed later in this section), likely due to micro-cracks and other flaws in the rock sample. Displacement data from the LVDT were not recorded during the test due to technical issues, leading to stress being plotted against time. The stress path, Mohr's circle, angle of internal friction, and cohesion of the sample are presented in the respective figures. The angle of internal friction for the multistage test was 48.12°, with cohesion of 0.83 MPa, while the single-stage test showed an angle of 44° and cohesion of 0.76 MPa (see **Table 9**). The rock exhibited diagonal shear failure along with some minor cracking.

Level 2 (50°C)

This level pertains to triaxial tests conducted on specimens treated at a temperature of 50°C. In the multistage triaxial test, the maximum axial stresses recorded at confining pressures of 2, 4, and 6 MPa were 45.74, 53.98, and 70.62 MPa, respectively (see **Table 8, Figures 4c and 4d**). For the three single-stage tests, peak axial stresses were observed at 56.34, 54.53, and 76.05 MPa at the corresponding confining pressures (see **Figure 5 e-h**). The variations in stress between the multistage and single-stage tests may be attributed to slight differences

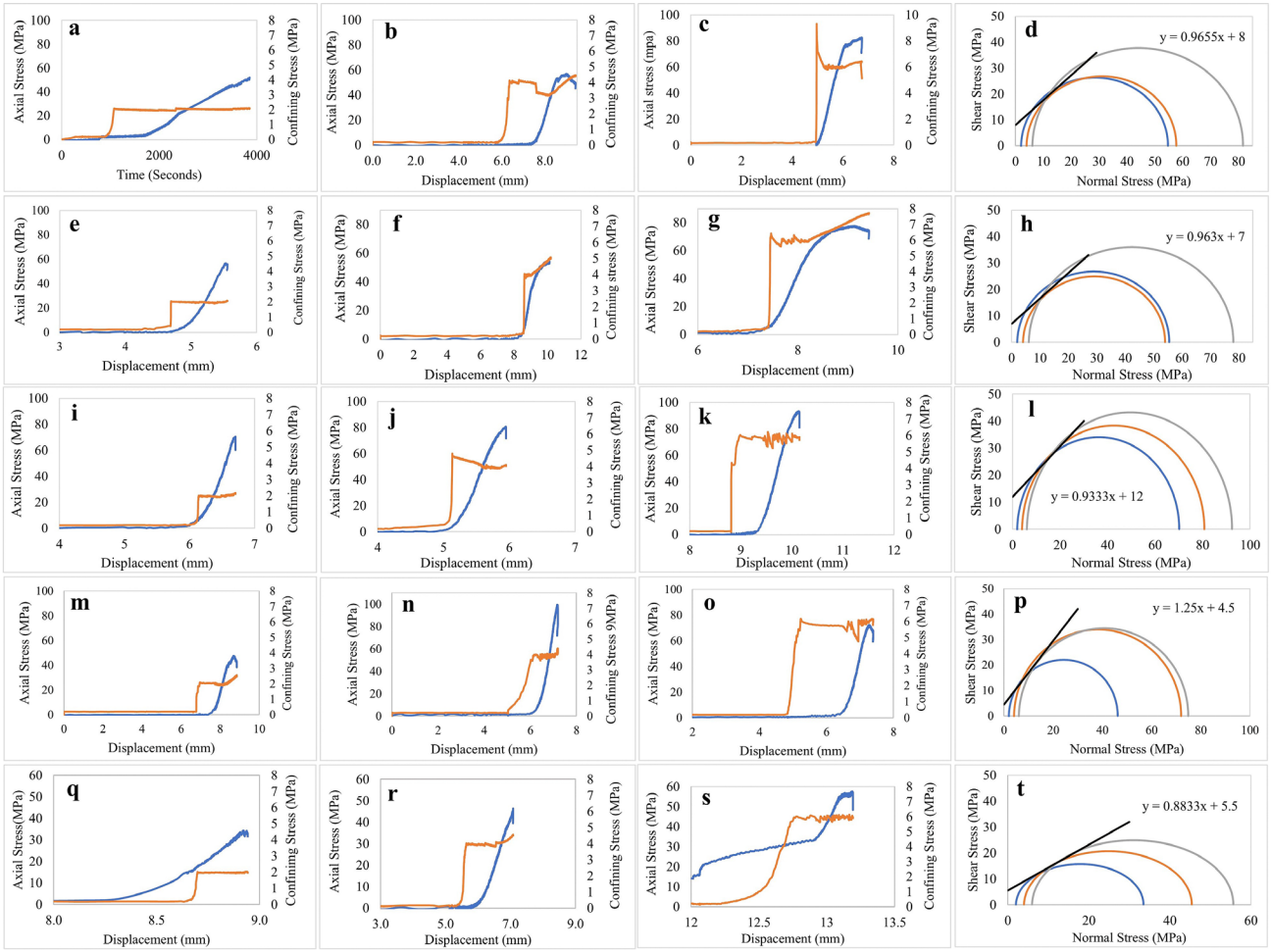

Figure 5 (a-t): shows the Stress paths of single-stage triaxial (SST) testing and Mohr's circle diagram at various temperatures. **a, b, c** show Stress paths of SST at 25°C while **d** shows Mohr's circle diagram; **e, f, g** show Stress paths of SST at 50°C while **h** shows Mohr's circle diagram; **i, j, k** show Stress paths of SST at 75°C while **l** shows Mohr's circle diagram; **m, n, o** show Stress paths of SST at 100°C while **p** shows Mohr's circle diagram; **q, r, s** show Stress paths of SST at 150°C while **t** shows Mohr's circle diagram. The blue line depicts axial stress, and the orange line shows confining stress.

in mineralogical composition, grain arrangement, and other flaws such as micro-cracks that impact the rock's strength. During this level, the multistage test measured the angle of internal friction at 39.35° and cohesion at 0.82 MPa, while the single-stage tests (see **Table 9**) recorded values of 43.92° and 0.76 MPa, respectively, indicating diagonal shear failure.

Level 3 (75°C)

Level 3 involved triaxial tests on specimens treated at 75°C. In the multistage test on a single specimen, maximum axial stresses were recorded as 52, 69.84, and 82.90 MPa at confining pressures of 2, 4, and 6 MPa, respectively (see **Table 8, Figures 4e and 4f**). For single-stage tests on three separate specimens, the peak axial stresses reached 69.92, 81.07, and 92.78 MPa (see **Table 9, Figures 5i-l**). The angle of internal friction was 46.97° in the multistage test and 43.02° in the single-stage tests, with cohesion values of 0.81 MPa and 0.75 MPa, respectively.

Level 4 (100°C)

For the triaxial test conducted at 100°C, the multistage test showed that the rock withstood maximum axial stresses of 68.29, 83.35, and 95 MPa at confining pressures of 2, 4, and 6 MPa, respectively (see **Table 8, Figures 4g and 4h**). In the single-stage tests, separate specimens reached maximum axial stresses of 46.43, 72.03, and 74.86 MPa at confining pressures of 2, 4, and 6 MPa, respectively (see **Table 9, Figures 5 m-p**). Typically, rock strength increases with higher confining pressures; however, in this case, the single-stage test at a 6 MPa confining pressure showed only a slight increase to 74.86 MPa compared to the 4 MPa result. This could be attributed to minor internal flaws and mineral thermal expansion from heat treatment, leading to thermal cracking and a reduction in strength. The angle of internal friction for the multistage test was 43.98° with cohesion of 0.83 MPa, while the single-stage test showed an internal friction angle of 51.3° and cohesion of 0.89 MPa.

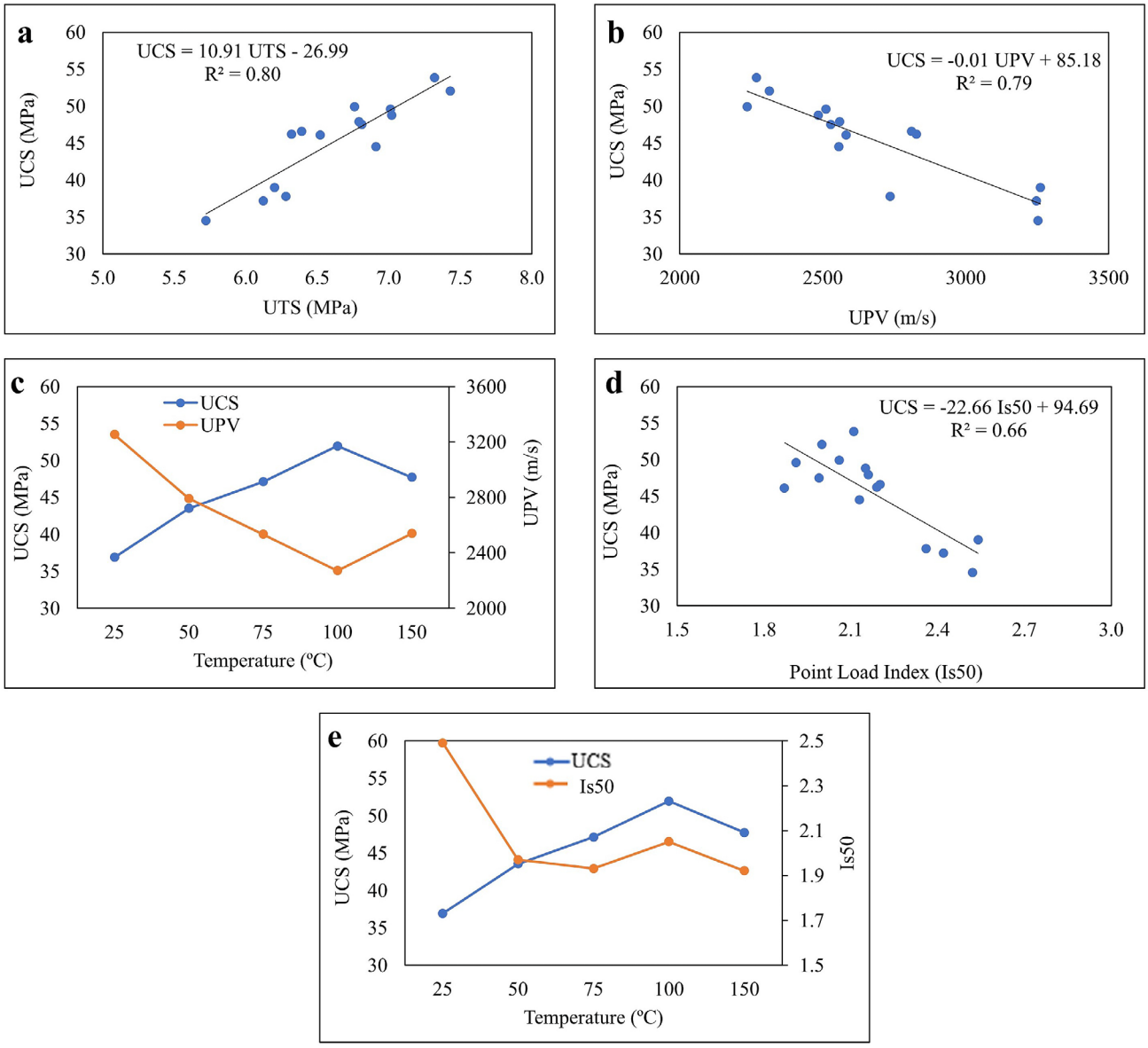

Figure 6 (a-e): Comparison of the UCS test with other tests. **a** shows the relationship between UCS and UTS for the studied samples. **b** shows the relationship between UCS and UPV. **c** shows the relationship between UCS, UPV and temperature. **d** shows the relationship between UCS and Is50. **e** shows the relationship between UCS, Is50 and temperature.

Level 5 (150°C)

At 150°C, one multistage and three single-stage triaxial tests were conducted on marble specimens under confining pressures of 2, 4, and 6 MPa. For the multistage test, the maximum axial stresses the rock withstood were 43.65, 49.77, and 58.32 MPa, respectively (see **Table 8, Figures 4i and 4j**). In the single-stage tests, three separate specimens reached maximum axial stresses of 33.51, 45.47, and 55.61 MPa (see **Table 9, Figures 5 r-t**). The general trend observed in this study is that marble strength increases with higher confining pressure from ambient temperature to 100°C, attributed to mineral thermal reactions that form new bonding agents, thereby enhancing rock strength (**Luo and Wang, 2011**). However, beyond 100°C, the strength begins to decline as mineral thermal expansion induces thermal cracking, reducing strength at 150°C (**Keshavarz et al., 2010**). The threshold temperature of 100°C is identified as the point of peak strength for the marble in this study area, aligning with previous findings (**Li et al., 2008**).

4.3. Variation of strength parameters with temperature

Figure 6 (a) illustrates the relationship between UCS and UTS for the studied samples treated at selected temperatures, showing a direct proportionality with R^2 = 0.80. **Figure 6 (b)** plots the compressive strength against UPV. Although previous studies have reported a positive trend; an inverse trend is observed with R^2 = 0.79. The reason is attributed to the heat treatment. **Figure 6 (c)**

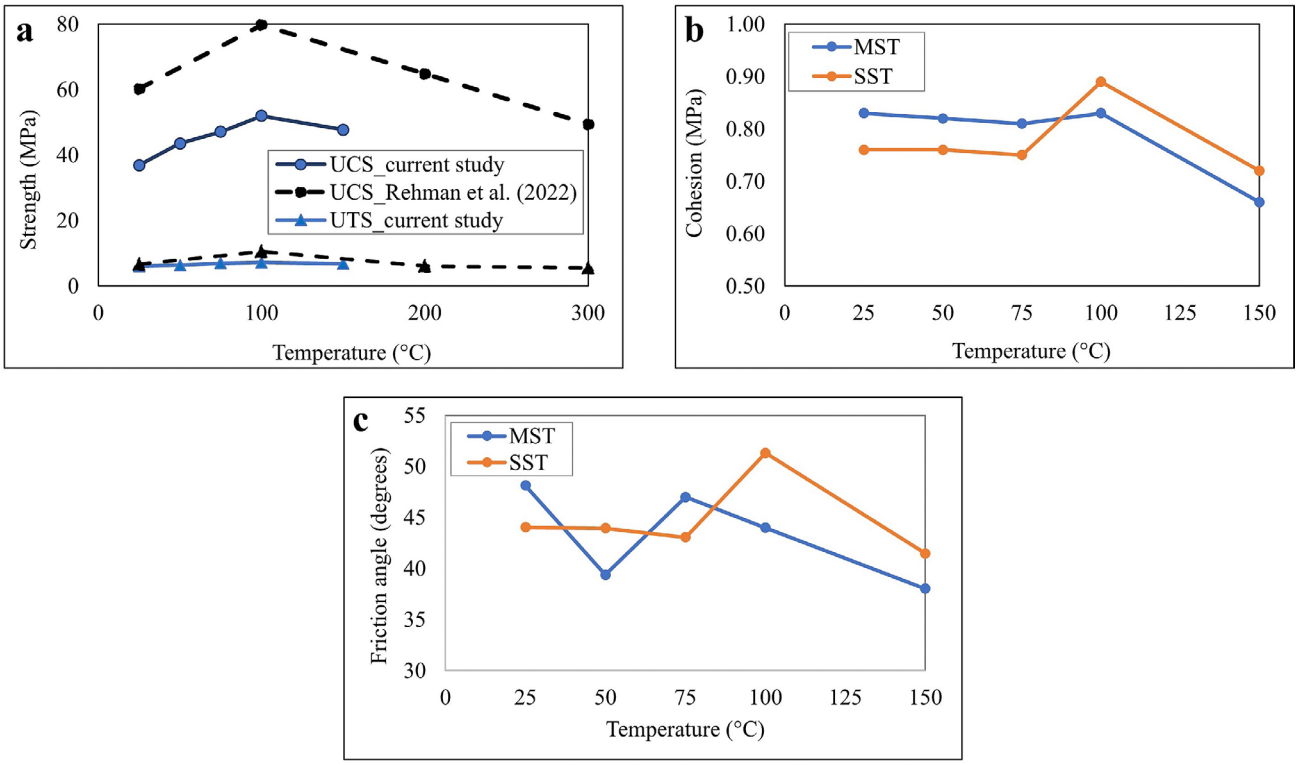

Figure 7 (a-c): Variation of strength parameters with temperature. **a** shows the variation of average strength with temperature. **b** shows the variation of average cohesion with temperature. **c** shows the variation of average friction angle with temperature.

depicts the UCS trend as temperature increases: UCS rises to 100°C, attributed to the grain boundary compactness and micro-fracture closure from calcite expansion, but decreases at 150°C as micro-fractures form due to differential strain. This trend is inversely mirrored in UPV values; as the temperature rises, free moisture vaporizes, creating voids and reducing UPV. **Figure 6 (d)** plots the compressive strength against the point load index (Is50) and an inverse trend is observed with $R^2 = 0.66$. Again, Is50 when plotted against UCS **Figure 6 (e)** shows it initially reduced from 25°C to 50°C and remained stable thereafter, with a slight decrease at 150°C.

Figure 7 presents the variation of strength parameters (UCS, UTS, cohesion, and friction angle) with temperature. UCS and UTS results align with **Rehman et al. (2022)**, who reported similar trends for Chitral and Khyber marbles (see **Figure 7 a**), showing an increase up to 100°C, followed by a decrease at 150°C (for both studies) and 300°C (**Rehman et al., 2022**). **Figures 7 b** and ⁊**7 c** show cohesion and friction angle variations at selected temperatures from SST and MST tests. Cohesion generally decreases with temperature for both SST and MST, except at 100°C. Similarly, the friction angle decreases with temperature, except for values recorded at 50°C (MST) and 100°C (MST). Further testing is recommended to establish a more reliable trend in the variation of cohesion and friction angle with temperature.

5. Conclusions

The marble deposits of the Nikani Ghar Formation in the Buner area were thoroughly analyzed for their physico-mechanical properties through conventional single and multistage triaxial compression tests at ambient and elevated temperatures. Following are the conclusions of this study:

The marbles meet acceptable standards for construction applications, including tunnels, highways, and bridges. The physico-mechanical properties of the marbles are comparable to global findings, with the exception of water absorption. Samples BM2 and BM4 exhibited higher water absorption, likely due to a higher proportion of hydrophilic minerals, which could impact their durability in specific environments.

Strength increased with temperature up to 100°C, attributed to mineral reactions forming new bonding agents, enhancing the rock‘s structural integrity. Beyond 100°C, a slight decrease in strength was observed at 150°C due to thermal expansion and the associated cracking.

A similar strength threshold was noted at 100°C, with degradation occurring at higher temperatures, emphasizing the importance of understanding thermal impacts in practical applications.

The mechanical properties of the marbles were strongly influenced by confining pressure. Peak strength

increased proportionally with confining pressure, demonstrating the marble's capability to withstand higher stresses in confined environments such as deep tunnels or underground structures.

Upon the above-mentioned conclusions, the following is recommended:

- Future studies should investigate the long-term durability of these marbles under cyclic thermal loading and varying environmental conditions, particularly for outdoor and high-temperature applications.
- Advanced microstructural techniques such as Scanning Electron Microscopy (SEM) and X-ray Diffraction (XRD) should be utilized to explore mineral transformations and their implications on strength and durability.
- It is highly recommended that engineers and designers consider the variations in water absorption and thermal behavior while selecting these marbles for specific applications, especially where thermal stability and low permeability are critical.

Acknowledgment

The authors would like to thank the National Centre of Excellence in Geology, University of Peshawar, Pakistan for providing laboratory facilities for this research work.

References

Ahmed, W., Ahmad, N., Janjuhah, H.T., Islam, I., Sajid, M., Kontakiotis, G. (2023): The Evaluation of Non-Destructive Tests for the Strength and Physical Properties of Granite, Marble, and Sandstone: A Case Study from North Pakistan. Quaternary, 6, 4. https://doi.org/10.3390/quat6010004

Ali, L., Ali, S., Khattak, S.A., Janjuhah, H.T., Kontakiotis, G., Hussain, R., Rukh, S., Shah, M.T., Bathrellos, G.D., Skilodimou, H.D. (2023): Distribution, Risk Assessment and Source Identification of Potentially Toxic Elements in Coal Mining Contaminated Soils of Makarwal, Pakistan: Environmental and Human Health Outcomes. Land, 12, 821. https://doi.org/10.3390/land12040821

Asif, A. R., Islam, I., Ahmed, W., Sajid, M., Qadir, A., Ditta, A. (2022); Exploring the potential of Eocene carbonates through petrographic, geochemical, and geotechnical analyses for their utilization as aggregates for engineering structures. Arabian Journal Geosciences, 15, 1–19. https://doi.org/10.1007/s12517-022-10383-0

Asif, A. R., Sajid, M., Ahmed, W., Nawaz, A. (2024): Weathering effects on granitic rocks in North Pakistan: petrographic insights, strength classifications, and construction suitability. Environmental Earth Sciences, 83, 351. https://doi.org/10.1007/s12517-022-10383-0

Asif A. R., Shah, S.S., Khan, J. (2021): The New Empirical Formulae for predicting the Unconfined Compressive Strength of limestone from Kohat Basin, Pakistan. Journal of Himalayan Earth Sciences, 54(1), 33.

Barone, G., Mazzoleni, P., Pappalardo, G., Raneri, S. (2015): Microtextural and microstructural influence on the changes of physical and mechanical proprieties related to salts crystallization weathering in natural building stones. The example of Sabucina stone (Sicily). Construction and building materials, 95, 355-365. https://doi.org/10.1016/j.conbuildmat.2015.07.131

Blyth, F. G. H., De Freitas, M. H. A. (1974): Geology for engineers: Hodder Education.

Bukhari, S.A.A., Basharat, M., Akgün, H., Sarfraz, Y., & Riaz, M.T. (2021): An evaluation of the geotechnical characteristics of Gahirat marble using empirical methods: A case study from the Chitral area, Khyber Pakhtunkhwa, North Pakistan. Journal of Himalayan Earth Science, 54(2).

Bukhari, S.A.A., Basharat, M., Janjuhah, H.T., Mughal, M.S., Goher, A., Kontakiotis, G., Vasilatos, C. (2023): Petrography and Geochemistry of Gahirat Marble in Relation to Geotechnical Investigation: Implications for Dimension Stone, Chitral, Northwest Pakistan. Applied Sciences, 13, 1755. https://doi.org/10.3390/app13031755

Cai, Y., Yu, S., Lu, Y. (2015): Experimental study on granite and the determination of its true strain-rate effect. Latin American Journal of Solids and Structures, 12, 675-694. https://doi.org/10.1590/1679-78251331

Calkins, J.A., Offield, T.W., Abdullah, S.K., & Ali, S.T. (1975): Geology of the southern Himalaya in Hazara, Pakistan, and adjacent areas (No. 716-C). US Govt. Print.

Chen, Y.L., Ni, J., Shao, W., Azzam, R. (2012): Experimental study on the influence of temperature on the mechanical properties of granite under uni-axial compression and fatigue loading. International Journal of Rock Mechanics and Mining Sciences, 56, 62-66. https://doi.org/10.1016/j.ijrmms.2012.07.026

Cheng, L., Houbin, L., Fengqiang, Y., Hanxiang, Y., Yingfeng, M.A. (2021): Study on the Mechanical Properties and Acoustic Response Characteristics of Marble in the Process of Triaxial Mechanical Loading. Journal of Southwest Petroleum University (Science & Technology Edition), 43(4) 1-10.

Coward, M.P., Butler, R.W.H., Chambers, A.F., Graham, R.H., Izatt, C. N., Khan, M.A., ... & Williams, M.P. (1988): Folding and imbrication of the Indian crust during Himalayan collision. Philosophical Transactions of the Royal Society of London. Series A, Mathematical and Physical Sciences, 326(1589), 89-116. https://doi.org/10.1098/rsta.1988.0081

Csuhanics, B. Debreczeni, A. (2013): Development of automatic control of multi-stage triaxial tests at the University of Miskolc. Geosciences and Engineering, 2(3), 37-43.

Ding, Q.L., Ju, F., Mao, X.B., Ma, D., Yu, B.Y., Song, S.B. (2016): Experimental investigation of the mechanical behavior in unloading conditions of sandstone after high-temperature treatment. Rock Mechanics and Rock Engineering, 49, 2641-2653. https://doi.org/10.1007/s00603-016-0944-x

Dipietro, J. A., Pogue, K. R., Lawrence, R. D., Baig, M. S., Hussain, A., & Ahmad, I. (1993). Stratigraphy south of the Main Mantle thrust, lower Swat, Pakistan. Geological Society, London, Special Publications, 74(1), 207-220. https://doi.org/10.1144/GSL.SP.1993.074.01.15

Dipietro, J.A. (1990): Stratigraphy, structure, and metamorphism near Saidu Sharif, Lower Swat, Pakistan.

Erguler, Z.A., & Ulusay, R. (2009): Water-induced variations in mechanical properties of clay-bearing rocks. International Journal of Rock Mechanics and Mining Sciences, 46(2), 355-370. https://doi.org/10.1016/j.ijrmms.2008.07.002

Fahad, M., Iqbal, Y., Riaz, M., Ubic, R., & Abrar, M. (2016): Geo-mechanical properties of marble deposits from the Nikani Ghar and Nowshera formations of the Lesser Himalaya, Northern Pakistan – a review. Himalayan Geology, 37, 17-27.

He, M.C., Miao, J.L., & Feng, J.L. (2010): Rock burst process of limestone and its acoustic emission characteristics under true-triaxial unloading conditions. International Journal of Rock Mechanics and Mining Sciences, 47(2), 286-298. https://doi.org/10.1016/j.ijrmms.2009.09.003

Hudson, J.A., Brown, E., Fairhurst, C. (2014): Rock testing and site characterization: Elsevier.

Hussain, A., Dipietro, J., Pogue, K., Ahmad, I. (2004): Geological map of the 43B degree sheet, NWFP, Pakistan.

Jaeger, J.C., Cook, N.G.W., & Zimmerman, R.W. (2007): Fundamentals of rock mechanics, 4th edn Blackwell. Maiden, MA, 475.

Janjuhah, H.T., Ishfaque, M., Mehmood, M.I., Kontakiotis, G., Shahzad, S.M., Zarkogiannis, S.D. (2021a): Integrated Underground Mining Hazard Assessment, Management, Environmental Monitoring, and Policy Control in Pakistan. Sustainability, 13, 13505. https://doi.org/10.3390/su132413505

Janjuhah, H.T., Kontakiotis, G., Wahid, A., Khan, D.M., Zarkogiannis, S.D., Antonarakou, A. (2021b): Integrated Porosity Classification and Quantification Scheme for Enhanced Carbonate Reservoir Quality: Implications from the Miocene Malaysian Carbonates. Journal of Marine Science and Engineering, 9, 1410. https://doi.org/10.3390/jmse9121410

Kamran, A., Ali, L., Ahmed, W., Zoreen, S., Jehan, S., Janjuhah, H.T., Vasilatos, C., Kontakiotis, G. (2022): Aggregate Evaluation and Geochemical Investigation of Limestone for Construction Industries in Pakistan: An Approach for Sustainable Economic Development. Sustainability, 14, 10812. https://doi.org/10.3390/su141710812

Kazmi, A.H., & Abbas, S.G. (2001): Metallogeny and mineral deposits of Pakistan. Islamabad: Orient Petroleum Inc, 88-150.

Keshavarz, M., Pellet, F.L., & Loret, B. (2010): Damage and changes in mechanical properties of a gabbro thermally loaded up to 1,000 C. Pure and Applied Geophysics, 167, 1511-1523. https://doi.org/10.1007/s00024-010-0130-0

Khan, J., Ahmed, W., Waseem, M., Ali, W., Rehman, I.u., Islam, I., Janjuhah, H.T., Kontakiotis, G., Bathrellos, G.D., Skilodimou, H.D. (2023): Lowari Tunnel Water Quality Evaluation: Implications for Tunnel Support, Potable Water Supply, and Irrigation in Northwestern Himalayas, Pakistan. Applied Sciences, 13, 8895. https://doi.org/10.3390/app13158895

Khan, J., Ahmed, W., Yasir, M., Islam, I., Janjuhah, H.T., Kontakiotis, G. (2022): Pollutants Concentration during the Construction and Operation Stages of a Long Tunnel: A Case Study of Lowari Tunnel, (Dir–Chitral), Khyber Pakhtunkhwa, Pakistan. Applied Sciences, 12, 6170. https://doi.org/10.3390/app12126170

Koroneos, E.G., Tassojannopoulos, A., & Diamantopoulou, A. (1980): On the mechanical and physical properties of ten Hellenic marbles. Engineering Geology, 16(3-4), 263-290. https://doi.org/10.1016/0013-7952(80)90019-8

Labeeb, M.S., Shahin, M., Alsawwaf, M., & Farouk, A. (2021): Point Load Index of Rocks Exposed to High Thermal Effect. Journal of Engineering Research, 5(1), 32-38. DOI: 10.21608/erjeng.2021.65559.1004

Li, D. W., Zhu, Z.D., Jiang, Z.J., & Qu, W.P. (2008): Microstructural investigation of mechanical characteristics of marbles under different temperatures. Journal of Hehai University (Natural Sciences), 36(3), 375-378.

Liu, S., & Xu, J. (2015): An experimental study on the physico-mechanical properties of two post-high-temperature rocks. Engineering Geology, 185, 63-70. https://doi.org/10.1016/j.enggeo.2014.11.013

Luo, J.A., & Wang, L. (2011): High-temperature mechanical properties of mudstone in the process of underground coal gasification. Rock mechanics and rock engineering, 44, 749-754. https://doi.org/10.1007/s00603-011-0168-z

Masri, M., Sibai, M., Shao, J.F., & Mainguy, M. (2014): Experimental investigation of the effect of temperature on the mechanical behavior of Tournemire shale. International Journal of Rock Mechanics and Mining Sciences, 70, 185-191. https://doi.org/10.1016/j.ijrmms.2014.05.007

Meng, L.B., Li, T.B., Cai, G.J. (2017): Temperature effects on the mechanical properties of slates in triaxial compression test. Journal of Mountain Science, 14(12), 2581-2588. https://doi.org/10.1007/s11629-016-4171-4

Nawaz, M., Ahmed, W., Yasir, M., Islam, I., Janjuhah, H.T., Kontakiotis, G., Antonarakou, A., Stouraiti, C. (2023): Petrographic and Geotechnical Features of Dir Volcanics as Dimension Stone, Upper Dir, North Pakistan. Geosciences, 13, 224. https://doi.org/10.3390/geosciences13080224

Okrusch, M., Bunch, T.E., & Bank, H. (1976): Paragenesis and petrogenesis of a corundum-bearing marble at Hunza (Kashmir). Mineralium Deposita, 11, 278-297. https://doi.org/10.1007/BF00203079

Peng, J., Rong, G., Cai, M., Yao, M.D., & Zhou, C.B. (2016): Physical and mechanical behaviors of a thermal-damaged coarse marble under uniaxial compression. Engineering Geology, 200, 88-93. https://doi.org/10.1016/j.enggeo.2015.12.011

Plevová, E., Kožušníková, A., Vaculíková, L., & Simha Martynková, G. (2010): Thermal behavior of selected Czech marble samples. Journal of thermal analysis and calorimetry, 101(2), 657-664. https://doi.org/10.1007/s10973-010-0907-5

Raza, M., Ahmed, W., Qazi, S., Azam, S., Sajid, M. (2024): Characterization of Buner marble from Pakistan for construction purposes. International Journal of Mining and Geo-Engineering, 58(2), 135-143. DOI: 10.22059/ijmge.2024.364177.595094

Rowley, D.B. (1996): Age of initiation of collision between India and Asia: A review of stratigraphic data. Earth and Planetary Science Letters, 145(1-4), 1-13. https://doi.org/10.1016/S0012-821X(96)00201-4

Sajid, M., Coggan, J., Arif, M., Andersen, J., & Rollinson, G. (2016): Petrographic features as an effective indicator for the variation in strength of granites. Engineering Geology, 202, 44-54. https://doi.org/10.1016/j.enggeo.2016.01.001

Shah, M.M., Ahmed, W., Ahsan, N., & Lisa, M. (2016): Fault-controlled, bedding-parallel dolomite in the middle Jurassic Samana Suk Formation in Margalla Hill Ranges, Khanpur area (North Pakistan): petrography, geochemistry, and petrophysical characteristics. Arabian Journal of Geosciences, 9, 1-18. https://doi.org/10.1007/s12517-016-2413-y

Shah, S.S.A., Asif, A.R., Ahmed, W., Islam, I., Waseem, M., Janjuhah, H.T., Kontakiotis, G. (2023): Determination of Dynamic Properties of Fine-Grained Soils at High Cyclic Strains. Geosciences, 13, 204. https://doi.org/10.3390/geosciences13070204

Shakirullah., Afridi, I.M. (2004): Mineral development profile of North West frontier Province and the role of directorate general mines and minerals in the minerals Resources development. Geological Bulletin University of Peshawar, 37, 139-154.

Silva, F.S., Ribeiro, C.E.G., Rodriguez, R.J.S. (2017): Physical and mechanical characterization of artificial stone with marble calcite waste and epoxy resin. Materials Research, 21, e20160377. https://doi.org/10.1590/1980-5373-MR-2016-0377

Tian, H., Mei, G., Jiang, G.S., & Qin, Y. (2017): High-temperature influence on mechanical properties of diorite. Rock Mechanics and Rock Engineering, 50, 1661-1666. https://doi.org/10.1007/s00603-017-1185-3

Ur Rehman, A., Ahmed, W., Azam, S., Sajid, M. (2022): Characterization and thermal behavior of marble from northwestern Pakistan. Innovative Infrastructure Solutions, 7, 1-8. https://doi.org/10.1007/s41062-021-00689-5

Wang, J.A., & Park, H.D. (2002): Fluid permeability of sedimentary rocks in a complete stress–strain process. Engineering geology, 63(3-4), 291-300. https://doi.org/10.1016/S0013-7952(01)00088-6

Yang, S.Q., Jiang, Y.Z., Xu, W.Y., Chen, X.Q. (2008): Experimental investigation on strength and failure behavior of pre-cracked marble under conventional triaxial compression. International Journal of Solids and Structures, 45(17), 4796-4819. https://doi.org/10.1016/j.ijsolstr.2008.04.023

Yang, S.Q., Tian, W.L., Jing, H.W., Huang, Y.H., Yang, X.X., Meng, B. (2019): Deformation and damage failure behavior of mudstone specimens under single-stage and multi-stage triaxial compression. Rock Mechanics and Rock Engineering, 52, 673-689. https://doi.org/10.1007/s00603-018-1622-y

Yang, S.Q., Xu, P., Ranjith, P.G., Chen, G.F., & Jing, H.W. (2015): Evaluation of creep mechanical behavior of deep-buried marble under triaxial cyclic loading. Arabian Journal of Geosciences, 8, 6567-6582. https://doi.org/10.1007/s12517-014-1708-0

Yaşar, E., & Erdoğan, Y. (2004): Estimation of rock physicomechanical properties using hardness methods. Engineering Geology, 71(3-4), 281-288. https://doi.org/10.1016/S0013-7952(03)00141-8

Yasir, M., Ahmed, W., Islam, I., Sajid, M., Janjuhah, H. T., & Kontakiotis, G. (2022): Composition, texture, and weathering controls on the physical and strength properties of selected intrusive igneous rocks from Northern Pakistan. Geosciences, 12(7), 273. https://doi.org/10.3390/geosciences12070273

Yavuz, H., Demirdag, S., & Caran, S. (2010): Thermal effect on the physical properties of carbonate rocks. International Journal of Rock Mechanics and Mining Sciences, 47(1), 94-103. https://doi.org/10.1016/j.ijrmms.2009.09.014

Yeats, R. S., & Hussain, A. (1987): Timing of structural events in the Himalayan foothills of northwestern Pakistan. Geological society of America bulletin, 99(2), 161-176. https://doi.org/10.1130/0016-7606(1987)99<161:TOSEIT>2.0.CO;2

Yu, J., Chen, S. J., Chen, X., Zhang, Y.Z., & Cai, Y.Y. (2015): Experimental investigation on mechanical properties and permeability evolution of red sandstone after heat treatments. Journal of Zhejiang University-SCIENCE A, 16, 749-759. https://doi.org/10.1631/jzus.A1400362

Zhang, J.C., Lin, Z.N., Dong, B., & Guo, R.X. (2021): Triaxial compression testing at constant and reducing confining pressure for the mechanical characterization of a specific type of sandstone. Rock Mechanics and Rock Engineering, 54, 1999-2012. https://doi.org/10.1007/s00603-020-02357-z

Zhu, Z., Tian, H., Mei, G., Jiang, G., Dou, B., & Xiao, P. (2021): Experimental investigation on mechanical behaviors of Nanan granite after thermal treatment under conventional triaxial compression. Environmental Earth Sciences, 80, 1-14. https://doi.org/10.1007/s12665-020-09326-3

SAŽETAK

Geomehaničko ponašanje mramora iz Bunera, Pakistan, kod povišene temperature: analiza čvrstoće u troosnome stanju jednofaznim i višefaznim pristupima

Ova studija istražuje efekt trodimenzionalnoga naprezanja na čvrstoću mramora iz okruga Buner, Khyber Pakhtunkhwa. Pruža usporednu analizu jednofaznih i višefaznih troosnih testova za procjenu čvrstoće mramora na sobnoj i povišenim temperaturama. Također ova studija ispituje fizičko-mehanička svojstva mramora kako bi se poboljšalo razumijevanje njegova ponašanja u različitim uvjetima. Prikupljeno je ukupno pet uzoraka mramora (BM1 do BM5). Iz tih je uzoraka izvađeno sedamdeset (70) jezgri za ispitivanje različitih fizičko-mehaničkih svojstava. Fizička ispitivanja uključuju specifičnu težinu, poroznost, apsorpciju vode i brzinu ultrazvučnih valova (UPV), a mehanička ispitivanja uključuju jednoosnu tlačnu čvrstoću (UCS), jednoosnu vlačnu čvrstoću (UTS), ispitivanje indeksa čvrstoće (PLT), a provedeno je i ispitivanje u troosnome stanju naprezanja. Fizička svojstva određena su za pet uzoraka (BM1 do BM5) odabranih iz skupnoga uzorka, dok su mehanička ispitivanja obavljena na preostalih 65 uzoraka. Opća znatna ujednačenost uočena je u vrijednostima svih fizičko-mehaničkih svojstava osim upijanja vode, koje je relativno veće u slučaju BM3 i BM5 (0,093 %) zbog povećane količine hidrofilnih minerala u tim uzorcima. Preostali uzorci jezgre tretirani su na povišenim temperaturama (50 °C, 75 °C, 100 °C i 150 °C). Mehanička svojstva UCS, UTS, PLT i troosna ispitivanja istražena su na uzorcima pri sobnoj (25 °C) i povišenoj temperaturi. U slučaju UCS-a i UTS-a utvrđeno je da se čvrstoća povećava s povećanjem temperature do granične temperature od 100 °C, nakon čega slijedi smanjenje na 150 °C. Slično, za parametre čvrstoće (koheziju i kut unutarnjega trenja) određene troosnim ispitivanjima ponovo je utvrđeno da je granična temperatura 100 °C nakon koje dolazi do smanjenja čvrstoće stijena. Povećanje čvrstoće pripisuje se toplinskim reakcijama minerala koje uzrokuju nove vezivne čimbenike i oni dovode do ojačanja stijena. S druge strane, smanjenje sa 100 °C na 150 °C dogodilo se zbog toplinske ekspanzije minerala što je rezultiralo toplinskim pucanjem i smanjenom čvrstoćom. Na temelju dobivenih rezultata, analize i usporedbe s međunarodnim standardima proučavane stijene mogu se koristiti za različite namjene pri podzemnoj gradnji.

Ključne riječi:
mramor, toplinsko djelovanje, fizičko-mehanička svojstva, jednofazno i višefazno troosno ispitivanje, toplinsko pucanje

Author's contribution

Asif Ali (MS Scholar), **Abdul Rahim Asif** (PhD, Lecturer), and **Muhammad Yasir** (PhD Scholar) contributed to the conceptualization, methodology, field investigation, data curation, and writing the original draft. **Waqas Ahmed** (PhD, Associate Professor), **Ihtisham Islam** (PhD, Lecturer) contributed to reviewing and editing, supervision, and funding acquisition. **Adnan Qadir** (MS Scholar) has guided geotechnical analysis. **Jehanzeb Khan** (PhD, Lecturer) contributed to field investigation, laboratory work, and data support. All co-authors made substantial contributions, read, and commented on several versions of the manuscript, and agreed with the contents of the manuscript.